Steady state and time-resolved spectroscopic studies on zinc(II) phthalocyanine in liposomes

Giuliana Valduga, Elena Reddi† and Giulio Jori
Department of Biology, University of Padova, Via Trieste 75, 35121 Padova (Italy)

Rinaldo Cubeddu, Paola Taroni and Gianluca Valentini
Centro Elettronica Quantistica e Strumentazione Elettronica, Consiglio Nazionale delle Ricerche, Politecnico di Milano, Piazza L. da Vinci 32, 20133 Milano (Italy)

(Received February 28, 1992; accepted May 25, 1992)

Abstract

Zinc(II) phthalocyanine (ZnPc), a potential second-generation photodynamic therapeutic agent for tumours, has been incorporated into small unilamellar vesicles (SUVs) (diameter, 52 nm) and large unilamellar vesicles (LUVs) (diameter, 84 nm) of dipalmitoyl-phosphatidylcholine (DPPC). Absorption spectroscopy, as well as steady state and time-resolved fluorescence emission studies, indicate that ZnPc is monomeric in SUVs at a stoichiometric concentration below 0.25 μM (corresponding to an actual endoliposomal concentration of about 0.5 mM), while in LUVs it is monomeric below 2 μM. The fluorescence lifetime of the monomer is 3–3.5 ns. Upon increasing the ZnPc concentration, aggregated derivatives are formed, which are characterized by shorter fluorescence lifetimes (1.2–1.5 ns; 0.4–0.6 ns). The possible implications of these observations for the photodynamic therapeutic efficiency of ZnPc are briefly discussed.

Keywords: Zinc(II) phthalocyanine, photosensitization, photodynamic therapy of tumours, fluorescence properties, liposomes.

1. Introduction

The incorporation of sparingly water-soluble photosensitizers into compartmentalized systems, such as liposomes, oil emulsions or cyclodextrins [1], allows their delivery to cell cultures, as well as their systemic injection into the bloodstream — hence the study of their photosensitizing behaviour *in vitro* and *in vivo* [2]. In particular, liposome-associated photosensitizers are accumulated by experimental tumours with a high degree of selectivity [3]. On these bases, it appears important to characterize the spectroscopic and photophysical properties of photosensitizers embedded in organized apolar structures. In aqueous dispersions of liposomes, hydrophobic photosensitizers are confined within the phospholipid bilayer; as a consequence, the volume actually available is only a small fraction of the whole medium and the local concentration of the photosensitizer in the bilayer can be orders of magnitude larger than the stoichiometric concentration, *i.e.* the concentration corresponding to a homogeneous distribution of

†Author to whom correspondence should be addressed.

the photosensitizer in the entire volume of the liposomal dispersion. How such a high concentration can affect the photophysical properties of the dye is a matter of investigation; several studies have been carried out on porphyrins (see, for a review, ref. 4) and, more recently, on phthalocyanines [5, 6] and porphycenes [7]. In all cases, complex fluorescence decays were observed; the results were interpreted either as reflecting the formation of aggregated photosensitizer species, the shorter lifetimes originating from dimers or oligomers, or as a consequence of the presence of different microenvironments for the photosensitizer in the bilayer.

In this paper we present a detailed characterization of absorption and fluorescence properties of zinc(II) phthalocyanine (ZnPc) in dipalmitoyl-phosphatidylcholine vesicles of different dimensions. The choice of this photosensitizer is justified by the fact that ZnPc has been recently proposed as a second-generation photosensitizing agent for tumour phototherapy because of its promising pharmacokinetic and phototherapeutic properties [8].

2. Materials and methods

2.1. Chemicals

ZnPc was purchased from Ciba–Geigy (Basle, Switzerland) and used as received. DL-α-dipalmitoyl-phosphatidylcholine (DPPC) was a product of Sigma (St. Louis, MO, USA). Disulphonated anthraquinone (AQDS) was obtained from Aldrich (Milwaukee, WI, USA). Octylviologen was prepared according to Ford and Tollin [9]. Other products and solvents were analytical-grade reagents and were used as received, without further purification.

2.2. Preparation of liposome dispersions

The liposome dispersions were prepared by the injection method of Kremer *et al.* [10]. This procedure allows the preparation of unilamellar phospholipid vesicles of pre-determined sizes through the injection of an ethanolic solution having different phospholipid concentrations into an aqueous buffered solution (0.01 M Tris-HCl, 0.1 M NaCl; pH = 7.4).

We prepared small unilamellar vesicles (SUVs) (radius, 26 nm) and large unilamellar vesicles (LUVs) (radius, 42 nm) of DPPC starting from 9.57 mM or 31.91 mM phospholipid solutions in absolute ethanol. The desired ZnPc concentrations in the liposomes were obtained by adding suitable volumes of a stock (1 mM) pyridine solution of the sensitizer to the ethanolic solution of DPPC. The ZnPc concentration in the liposomal dispersions was checked by diluting the suspensions with an excess of pyridine and measuring the absorption spectrum ($\epsilon = 241\,000\ M^{-1}\ cm^{-1}$ at 673 nm) [8].

2.3. Steady state absorption and fluorescence measurements

Absorption spectra were recorded with a Lambda 5 Perkin–Elmer spectrophotometer, while fluorescence emission spectra (excitation at 600 nm) were obtained with an MPF 4 spectrophotofluorometer. Before measurement, the liposome dispersions were diluted with buffer to give an absorbance lower than 0.1 at 673 nm, thus minimizing inner filter effects and fluorescence reabsorption. Fluorescence yields of ZnPc at different concentrations were estimated relative to the yield of 0.1 μM ZnPc in DPPC SUVs taken as 100% by integrating the area under the fluorescence peak and correcting for the absorbance at 600 nm.

In fluorescence quenching experiments, small volumes of an aqueous stock solution of AQDS or octylviologen were added stepwise to 2 ml of a liposome dispersion

containing 0.25 μM ZnPc. The data were analysed in terms of the modified Stern–Volmer equation [11]:

$$\frac{F_0}{F_0 - F} = \frac{1}{Q}\left(1 \Big/ \sum_i f_i k_{Qi}\right) + \sum_i k_{Qi} \Big/ \sum_i f_i k_{Qi}$$

where F_0 and F are the fluorescence intensities at 678 nm in the absence and in the presence respectively of the quencher, Q is the quencher concentration, and f_i and k_{Qi} represent the fractional fluorescence and the fluorescence quenching constant respectively for the ith ZnPc molecule. Plotting $F_0/(F_0 - F)$ against $1/Q$, one can calculate $\Sigma_i k_{Qi} = k_Q$, the effective quenching constant, from the intercept-to-slope ratio of the linear part of the plot, while the reciprocal of the intercept gives $\Sigma_i f_i k_{Qi} / \Sigma_i k_{Qi} = f_a$, the effective fraction of quencher-accessible fluorescence.

2.4. Time-gated fluorescence measurements

A mode-locked argon ion laser tuned at 364 nm, with a pulse duration of about 150 ps, was used as the excitation source. The repetition rate was reduced to about 700 kHz by means of an acousto-optic pulse picker.

The detection of the fluorescence photons was provided by a microchannel-plate photomultiplier connected to an electronic chain for time-correlated single-photon counting. This system was extended through a home-built acquisition unit for the selection of the time-to-amplitude converter output pulses. The whole apparatus has been described in detail in ref. 12. It allowed the simultaneous acquisition of the time-integrated emission spectrum, two time-gated spectra and the fluorescence decay curve. The emission spectra were collected in the 620–700 nm range in 2 or 5 nm steps. The overall time resolution of the system was about 150 ps. The fluorescence waveforms were analysed by a non-linear least-squares fitting procedure. The weighted residuals and their autocorrelation function were used to judge the obtained results. Different measurements provided variations in the time decays from 50 to 300 ps, depending on the decay value, and the fluctuations in the relative amplitude were within a few per cent.

Time-gated data were collected from the same samples as considered for steady state fluorescence measurements. Preliminary fitting of the fluorescence decay curves obtained at several ZnPc concentrations indicated the presence of at most three exponential components, characterized by lifetimes of 3–3.5 ns, 1.2–1.5 ns and 0.4–0.6 ns respectively.

On the basis of these results, the following gate parameters were selected: an undelayed gate, 500 ps wide, and an 8 ns-delayed gate, 6 ns wide. The first choice was made to enhance the contribution of the fast-decaying species, while the 8 ns delay allowed us to isolate the emission of the long-living component.

The time-integrated spectra were obtained by counting all the fluorescence photons falling within approximately the first 25 ns after the excitation pulse. Therefore they are actually the same as continuous-wave emission spectra.

3. Results

3.1. Steady state measurements

Figure 1 shows the dependence of the absorbance at the absorption maximum (673 nm) on ZnPc concentration in SUVs and LUVs. The plot is linear up to a 2 μM stoichiometric ZnPc concentration; in this range the extinction coefficient is

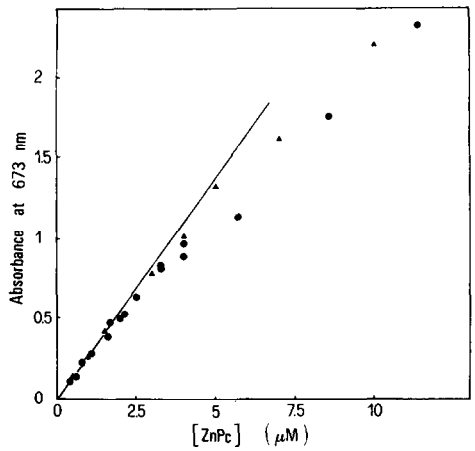

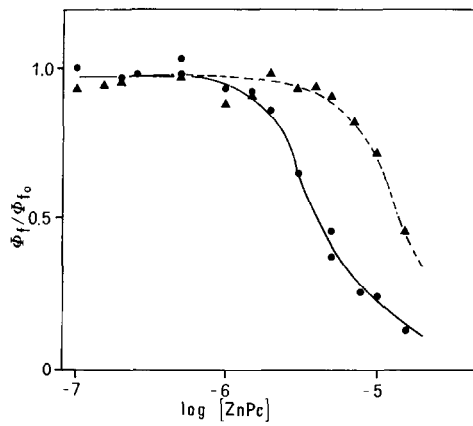

Fig. 1. Variation in the 673 nm absorbance as a function of stoichiometric ZnPc concentration in aqueous dispersions of DPPC SUVs (●) and DPPC LUVs (▲).

Fig. 2. Relative fluorescence yield as a function of ZnPc stoichiometric concentration in aqueous dispersions of DPPC SUVs (●) and in DPPC LUVs (▲).

identical with that found for ZnPc in pyridine. A deviation from linearity occurs at higher ZnPc concentrations and is accompanied by slight changes in the spectral shape; for the highest ZnPc concentrations in SUVs a broadening of the main band and the appearance of a shoulder at about 680 nm are observed. For DPPC LUVs both the deviation from the linearity and the changes in the spectrum occur at higher ZnPc concentrations.

The ZnPc fluorescence yield in the liposomal systems decreases with increasing sensitizer concentration, as shown in Fig. 2. The addition of aqueous octylviologen or AQDS to SUV dispersions causes a quenching of the ZnPc fluorescence; however, the Stern–Volmer plot tends to give a negative deviation from linearity, suggesting a heterogeneous distribution of the fluorophore in the vesicle. A recalculation of the data according to the modified Stern–Volmer equation yields k_q values of 7.42×10^3 M^{-1} for AQDS and 2.86×10^5 M^{-1} for octylviologen; in both cases, only a small fraction (13–14%) of the sensitizer molecules is accessible to the quenchers.

3.2. Time-gated measurements

The fluorescence decay of ZnPc in the stoichiometric concentration range 0.05–0.25 μM in DPPC SUVs is best fitted by a single-exponential curve with a time constant of 3.5 ns (Table 1), as also obtained for ZnPc in absolute ethanol. This lifetime slightly decreased upon increasing the ZnPc concentration. A Stern–Volmer plot of $1/\tau_1$ *vs.* local concentration of ZnPc is linear and gives an apparent $k_q=6.5\times10^9$ M^{-1} s^{-1}. At a ZnPc concentration of 0.5 μM (corresponding to the end of the plateau region for SUVs in Fig. 1) a second exponential component with a time constant of about 1.25 ns is observed. Its relative amplitude increases with increasing concentration, being approximately 46% at 2 μM. Upon further increasing the concentration the relative amplitudes of both components decrease and a third short-living (about 0.5 ns) exponential component appears, which becomes predominant above 5 μM.

At all the concentration values considered, time-gated emission spectra of ZnPc were also measured to evaluate the contributions of the different exponential components

TABLE 1

Fluorescence lifetimes τ of zinc(II) phthalocyanine and their relative amplitudes A at different phthalocyanine concentrations in dipalmitoyl-phosphatidylcholine small unilamellar vesicles

ZnPc (μM)	τ_1 (ns)	A_1 (%)	τ_2 (ns)	A_2 (%)	τ_3 (ns)	A_3 (%)
0.05	3.53	100.00				
0.25	3.45	100.00				
0.50	3.45	83.92	1.35	16.08		
1.00	3.23	75.99	1.15	24.01		
2.00	3.15	53.84	1.26	46.16		
3.50	3.01	33.70	1.27	36.70	0.55	29.60
5.00	2.86	28.21	1.22	29.52	0.46	42.28
7.50	2.59	12.03	1.41	29.46	0.45	58.51

by setting the first gate at 0 ns delay (0.5 ns wide) and the second gate at 8 ns delay (6 ns wide). The time-integrated spectra show a concentration-dependent increase in the emission intensity on the red side of the spectrum (Fig. 3(a)). This increase is more relevant in the undelayed spectra (Fig. 3(b)), while the delayed spectra remain unchanged at all the concentrations (Fig. 3(c)) and overlap the spectrum of ZnPc in the 0.05–0.25 μM range. Since the delayed spectrum is mostly influenced by the 3.5 ns component, the observed spectral modifications can be related to the presence of the fast and intermediate components. A similar behaviour occurs for ZnPc in DPPC LUVs, although the intermediate and fast components are detected at higher phthalocyanine concentrations (Table 2): the intermediate and fast components appear at about 2 μM and 5 μM respectively, while even at the highest ZnPc concentration considered (12 μM) the slow component is dominant. Some differences are also detected in the time-gated spectra. A spectral broadening to the red is present above 2 μM ZnPc and is more relevant with respect to the SUV liposomes. Moreover, upon increasing the ZnPc concentration, this modification is still apparent in the delayed spectra, although to a lesser extent (Fig. 4).

4. Discussion

Our results indicate that ZnPc incorporated in DPPC SUVs and LUVs is monomeric at stoichiometric concentrations below 0.5 μM and 2 μM respectively, as suggested by the single-exponential fluorescence decay, while some types of intermolecular interaction (including aggregation) appear to occur at higher ZnPc concentrations. The evidence indicating ZnPc aggregation includes (i) the deviation of the Beer–Lambert plot from linearity which is accompanied by a broadening of the absorption spectrum, as is typical of aggregated phthalocyanine species [5], (ii) the decrease in fluorescence quantum yield and the appearance of short-lived emitters, both phenomena having been previously reported for several aggregated metallophthalocyanines [13] and (iii) the red broadening of the emission spectrum observed in undelayed time-gated measurements due to the contribution of fast-decaying species; this parallels the above-mentioned broadening of the absorption spectrum.

Alternative interpretations ascribing the various fluorescence lifetimes to ZnPc molecules located in different endoliposomal sites appear to be less likely. In principle,

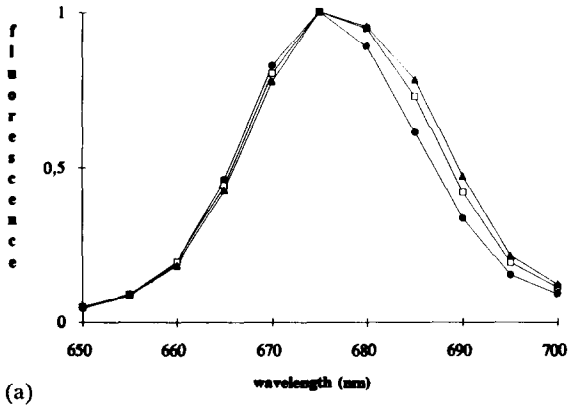

(a)

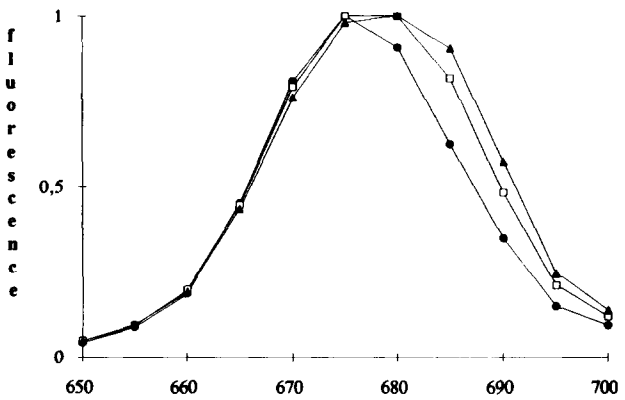

(b)

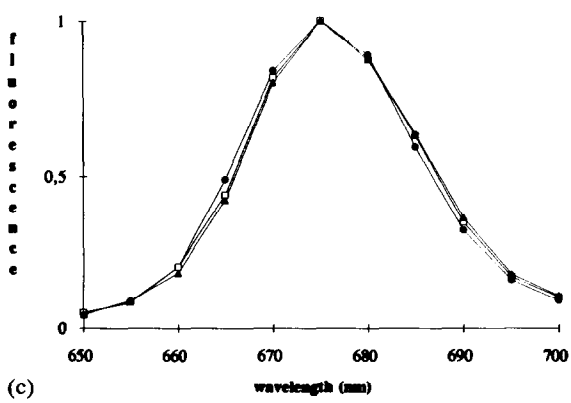

(c)

Fig. 3. Emission spectra ((a) time-integrated spectrum; (b) time-gated spectrum, undelayed, 500 ps wide; (c) time-gated spectrum, 8 ns delayed, 6 ns wide) of ZnPc in DPPC SUVs at different concentrations: –●–, 0.5 μM; –□–, 2 μM; –▲–, 3.5 μM.

TABLE 2

Fluorescence lifetimes τ of zinc(II) phthalocyanine and their relative amplitudes A at different phthalocyanine concentrations in dipalmitoyl-phosphatidylcholine large unilamellar vesicles

ZnPc (μM)	τ_1 (ns)	A_1 (%)	τ_2 (ns)	A_2 (%)	τ_3 (ns)	A_3 (%)
0.10	3.44	100.00				
0.50	3.77	100.00				
1.00	3.28	100.00				
2.00	3.50	66.14	2.10	33.86		
5.00	3.23	50.56	1.52	39.30	0.22	10.13
7.50	3.10	48.71	1.24	34.93	0.33	16.36
10.00	3.22	36.80	1.73	38.73	0.49	24.48
12.00	2.94	43.40	1.27	33.79	0.36	22.81

it is possible to hypothesize that ZnPc first occupies high affinity or most readily accessible sites, whereas other sites can be occupied only in the presence of relatively large phthalocyanine concentrations. However, such a picture can hardly fit into the whole framework of our spectroscopic data, in particular the concentration dependence of the absorption and steady state or time-resolved fluorescence properties. Although the fluorescence quenching results would also indicate some heterogeneity in the endoliposomal distribution of ZnPc, it is important to emphasize that at least two populations of liposome-bound phthalocyanine (one is accessible and the other is inaccessible to octylviologen and anthraquinone disulphonate) are observed also when fluorescence decay measurements indicate the presence of a single species. Consequently, the presence of multiple fluorescence lifetimes and the heterogeneity in ZnPc endoliposomal distribution, as suggested by fluorescence quenching studies, appear to be unrelated events.

On the basis of the information available in the literature on the fluorescence properties of polycyclic dyes [13–18], we ascribe the long-lived transient (3–3.5 ns) to monomeric ZnPc; the transients with shorter lifetimes (1.2–1.5 ns and 0.4–0.5 ns) are due to aggregated derivatives. At the present stage of our investigations, we are unable to decide whether the two lifetimes are to be assigned to a dimer and a higher oligomer, or to two dimers having different geometries ("face to face" or side by side). The possibility also exists of different types of electronic interaction between the π electron clouds of ZnPc molecules having different mutual orientations in the phospholipid bilayer. The presence of aggregated ZnPc in the liposomal phospholipid bilayer is probably related to the restricted motility of the tetraazaisoindole derivative in the hydrocarbon-type milieu and its high local concentration, which enhance the probability of intermolecular interactions. In fact, steady state fluorescence quenching experiments indicate that only a small fraction of liposome-bound ZnPc is accessible to water-soluble quenchers; thus most phthalocyanine molecules must be deeply buried in the core of the phospholipid chains. Therefore the fact that ZnPc aggregation appears to occur at higher phthalocyanine concentrations in LUVs than in SUVs reflects the larger volume available in the phospholipid bilayer of the former liposomes. Under our experimental conditions, the average number of phospholipid molecules per liposome is 25 340 in SUVs and 60 670 in LUVs [10]. If one estimates the average number of ZnPc molecules per vesicle, a close correspondence between the fluorescence yields in the two liposomes at identical phthalocyanine-to-phospholipid ratios is observed;

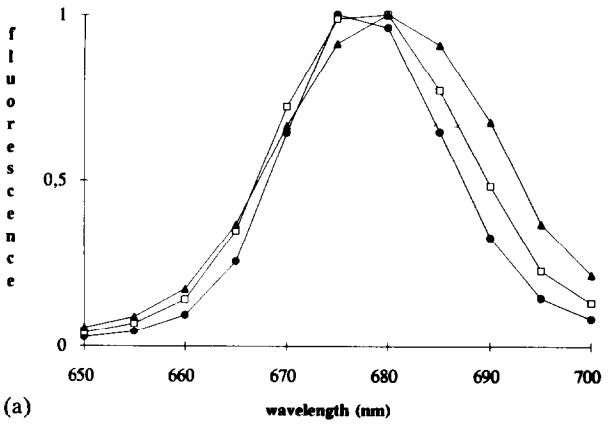

(a)

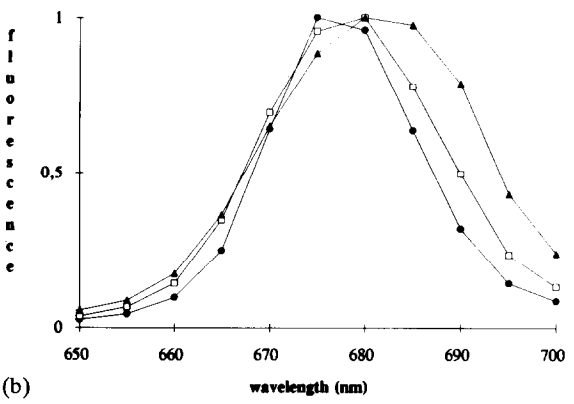

(b)

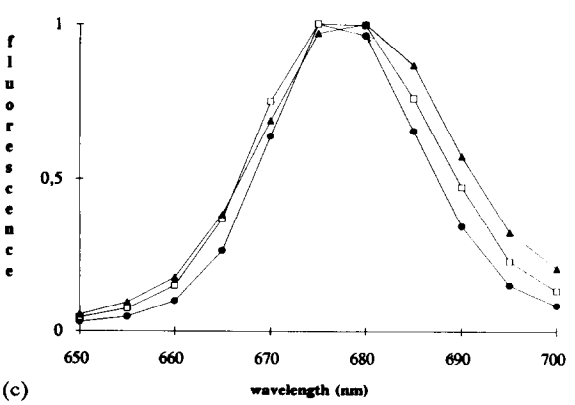

(c)

Fig. 4. Emission spectra ((a) time-integrated spectrum; (b) time-gated spectrum, undelayed, 500 ps wide; (c) time-gated spectrum, 8 ns delayed, 6 ns wide) of ZnPc in DPPC LUVs at different concentrations: –●–, 0.5 μM; –□–, 2 μM; –▲–, 12 μM.

in particular, the appearance of the second and third faster-decaying transients takes place at ZnPc-to-DPPC ratios of about 1 to 1200 and about 1 to 300 in both cases.

If our interpretation is correct, one must draw the conclusion that, when ZnPc is injected *in vivo* after incorporation into DPPC SUVs, a substantial aliquot of the phthalocyanine is in an aggregated state. This is known to decrease its photosensitizing activity [13]. However, DPPC liposome-administered ZnPc has been reported to be an efficient phototherapeutic agent for experimental tumours [8]. Therefore the possibility exists that ZnPc undergoes monomerization either when the liposomal particles interact with serum lipoproteins or upon delivery of the phthalocyanine from the lipoproteins to the malignant cells. A similar process has been proposed to occur for some oligomeric components of Photofrin II, the mixture of haematoporphyrin derivatives at present used in clinical photodynamic therapy of tumours [19].

Acknowledgments

This work received financial support from Consiglio Nazionale delle Ricerche (Italy) under the special project "Tecnologie Elettroottiche", Grant 90.00227.

References

1 G. M. Garbo and A. R. Morgan, Delivery systems for hydrophobic drugs, *J. Photochem. Photobiol. B: Biol., 1* (1988) 494–495.
2 G. Jori, Photosensitized processes in vivo: proposed phototherapeutic applications, *Photochem. Photobiol., 52* (1990) 439–443.
3 G. Jori and E. Reddi, Strategies for tumour targeting by photodynamic sensitizers, in D. Kessel (ed.), *Photodynamic Therapy of Neoplastic Disease,* CRC Press, Boca Raton, FL, 1990, pp. 117–130.
4 M. A. J. Rodgers, The photoproperties of porphyrins in model biological environments, in G. Jori and C. Perria (eds.), *Photodynamic Therapy of Tumors and Other Diseases,* Libreria Progetto Editore, Padova, 1985, pp. 22–35.
5 J. E. van Lier and J. D. Spikes, The chemistry, photophysics and photosensitizing properties of phthalocyanines, *Photosensitizing Compounds: their Chemistry, Biology and Clinical Use, Ciba Foundation Symp., 146,* Wiley, Chichester, 1989, pp. 17–26, 193–207.
6 G. Valduga, S. Nonell, E. Reddi, G. Jori and S. E. Braslavsky, The production of singlet molecular oxygen by zinc(II)-phthalocyanine in ethanol and unilamellar vesicles. Chemical quenching and phosphorescence studies, *Photochem. Photobiol., 48* (1988) 1–5.
7 R. W. Redmond, G. Valduga, S. Nonell, S. E. Braslavsky, K. Schaffner, E. Vogel, K. Pramod and M. Kocher, The photophysical properties of porphycene incorporated in small unilamellar vesicles, *J. Photochem. Photobiol. B: Biol., 3* (1989) 193–207.
8 E. Reddi, C. Zhou, R. Biolo, E. Menegaldo and G. Jori, Liposome- or LDL-administered Zn(II)-phthalocyanine as a photodynamic agent for tumours. I. Pharmacokinetic properties and phototherapeutic efficiency, *Br. J. Cancer, 61* (1990) 407–411.
9 W. E. Ford and G. Tollin, Chlorophyll photosensitized electron transfer in phospholipid bilayer vesicle systems: correlations between kinetic parameters and solubilities of viologen acceptors, *Photochem. Photobiol., 43* (1986) 319–330.
10 J. M. H. Kremer, M. W. J. von der Esker, C. Pathmamanoharan and P. H. Wiersma, Vesicles of variable diameter prepared by a modified injection method, *Biochemistry, 16* (1977) 3932–3935.
11 S. S. Lehrer, Solute perturbation of protein fluorescence. The quenching of tryptophyl fluorescence of model compounds and of lysozyme by iodide ion, *Biochemistry, 10* (1971) 3254–3263.

12 R. Cubeddu, F. Docchio, W. Q. Liu, R. Ramponi and P. Taroni, A system for time-resolved laser fluorescence spectroscopy with multiple picosecond gating, *Rev. Sci. Instrum., 59* (1988) 2254–2259.
13 J. D. Spikes, Phthalocyanines as photosensitizers in biological systems and for the photodynamic therapy of tumors, *Photochem. Photobiol., 43* (1986) 691–699.
14 A. Andreoni, R. Cubeddu, S. De Silvestri, P. Laporta, G. Jori and E. Reddi, Hematoporphyrin derivative: experimental evidence for aggregated species, *Chem. Phys. Lett., 88* (1982) 33–36.
15 A. Andreoni, R. Cubeddu, S. De Silvestri, G. Jori, P. Laporta and E. Reddi, Time-resolved fluorescence studies of hematoporphyrin in different solvent systems, *Z. Naturforsch., 38c* (1983) 83–89.
16 D. Kessel, Probing the structure of HpD by fluorescence spectroscopy, *Photochem. Photobiol., 50* (1989) 345–350.
17 E. Unsold, C. Ell, D. Jocham, R. Sroka and S. Stocker, Quantitative and comparative study of hematoporphyrin-derived photosensitizers in a murine tumor model, *Lasers Med. Sci., 5* (1990) 309–310.
18 G. Bottiroli, A. C. Croce, R. Ramponi and P. Vaghi, Distribution of di-sulfonated aluminium phthalocyanine and photofrin II in living cells: a comparative fluorometric study, *Photochem. Photobiol., 55* (1992) 575–585.
19 D. Kessel, Photosensitization with derivatives of hematoporphyrin, *Int. J. Radiat. Biol., 49* (1986) 901–907.